RESEARCH ARTICLE | MARCH 20 2024

The large magnetocaloric effect in GdErHoCoM (M = Cr and Mn) high-entropy alloy ingots with orthorhombic structures



Special Collection: Era of Entropy: Synthesis, Structure, Properties, and Applications of High-Entropy Materials

Xuejiao Wang 💿 ; Shuotong Zong 🔀 💿 ; Yan Zhang; Zhaojun Mo 💿 ; Junwei Qiao 🔀 💿 ; Peter K. Liaw 💿



Appl. Phys. Lett. 124, 122412 (2024) https://doi.org/10.1063/5.0196758





Articles You May Be Interested In

Magnetocaloric effect and magnetic phase transition in Ho₃Co

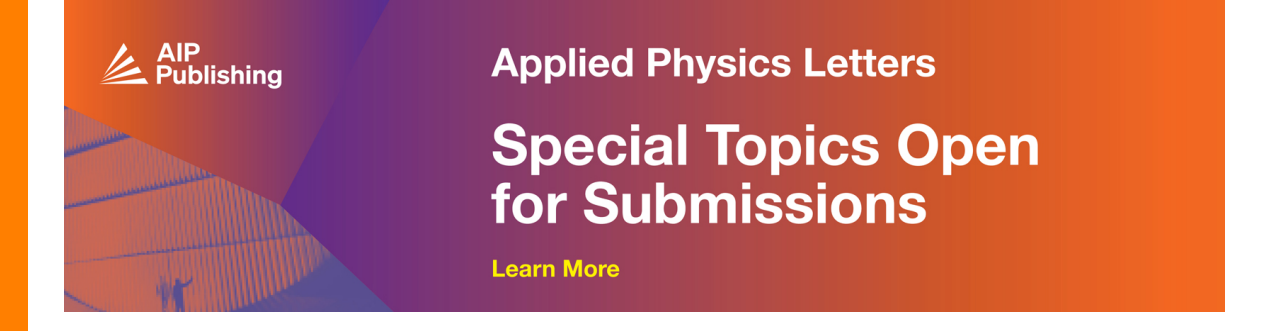
J. Appl. Phys. (April 2011)

New magnetic configuration in paramagnetic phase of HoCo₂

J. Appl. Phys. (February 2012)

Abstract: Magnetic properties of rare earth-transition metal amorphous thin films

J. Vac. Sci. Technol. (January 1975)





The large magnetocaloric effect in GdErHoCoM (M = Cr and Mn) high-entropy alloy ingots with orthorhombic structures

Cite as: Appl. Phys. Lett. 124, 122412 (2024); doi: 10.1063/5.0196758 Submitted: 9 January 2024 · Accepted: 10 March 2024 · Published Online: 20 March 2024







Xuejiao Wang, ҧ Shuotong Zong,^{2,3,a)} 🕞 Yan Zhang,^{2,3} Zhaojun Mo,⁴ 🕞 Junwei Qiao,^{1,a)} 🕞 and Peter K. Liaw⁵ 🕞





AFFILIATIONS

- School of Materials Science and Engineering, Taiyuan University of Technology, Taiyuan 030024, China
- 2 School of Materials Science and Engineering, Taiyuan University of Science and Technology, Taiyuan 030024, China
- 3 Laboratory of Magnetic and Electric Functional Materials and the Applications, The Key Laboratory of Shanxi Province, Taiyuan 030024, China
- 4 Key Laboratory of Rare Earths, Ganjiang Innovation Academy, Chinese Academy of Sciences, Ganzhou 341119, China

Note: This paper is part of the APL Special Collection on Era of Entropy: Synthesis, Structure, Properties, and Applications of High Entropy Materials.

^{a)}Authors to whom correspondence should be addressed: zongshuotong@tyust.edu.cn and qiaojunwei@gmail.com

ABSTRACT

High-entropy alloys (HEAs) with significant magnetocaloric effects (MCEs) have attracted widespread attention due to their potential magnetic refrigeration applications over a much more comprehensive temperature range with large refrigerant capacity (RC). However, most of them are metallic glasses (MGs) with problems of limited size, resulting in the difficulty of further applications. Therefore, research on HEAs with crystalline structures and giant MCE is urgently needed. In this paper, GdErHoCoM (M = Cr and Mn) rare-earth HEA ingots with orthorhombic structures are developed, and their magnetic behavior and MCE are studied in detail. Phase investigations find that the main phase of GdErHoCoM ingots is probably (GdErHo)Co with an orthorhombic Ho₃Co-type structure of a space group of Pnma. The secondary phases in GdErHoCoCr and GdErHoCoMn are body-center-cubic Cr and Mn-rich HoCo2-type phases, respectively. Magnetic investigations reveal that both ingots undergo a first-order magnetic phase transition below their respective Neel temperatures. Above their respective Neel temperatures, a second-order transition is observed. The Neel temperatures are 40 and 56 K for GdErHoCoCr and GdErHoCoMn, respectively. Additionally, the GdErHoCoCr and GdErHoCoMn ingots exhibit maximum magnetic entropy changes and RC values of 12.29 J/kg/K and 746 J/kg and 10.13 J/kg/K and 606 J/kg, respectively, under a magnetic field of 5 T. The ingots GdErHoCoM (M = Cr and Mn) show excellent MEC properties and can be manufactured easily, making them promising for magnetic refrigerant applications.

Published under an exclusive license by AIP Publishing. https://doi.org/10.1063/5.0196758

The magnetic refrigeration technology, using the magnetocaloric effect (MCE) for refrigeration, has attracted widespread attention due to its many extraordinary advantages, such as high efficiency, environmental friendliness, and great silence. 1-3 To achieve refrigeration, magnetic refrigeration materials go through periodic heat absorption and release during demagnetization and magnetization processes; therefore, materials with a large MCE and refrigerant capacity (RC) are in urgent demand for the development of magnetic refrigeration technology. 4,5 In recent years, high-entropy alloys (HEAs), 6,7 which contain five or more elements with equal or near-equal atomic percentages, have exhibited outstanding magnetocaloric properties due to their complicated structures,⁸ diverse components,^{9–11} MCE, and RC.¹² Among them, the rare-earth-based (RE) HEAs, such as GdTbHoErLaY, ¹⁶ RErHoTb (R = Gd and Dy), ¹⁴ ScGdTbDyHo, ¹⁷ and HoErCoAlR (R = Gd, Dy, and Tm), ¹³ have drawn the attention due to their large MCE over a much wide temperature range with large RC. These RE-HEAs can be divided into metallic glasses¹⁸ and crystalline according to their crystallization. Until now, most known large MCE-HEAs are metallic glasses (MGs), including RErHoTb (R = Gd and Dy), ScGdTbDyHo, and HoErCoAlR (R = Gd, Dy, and Tm). Among

 $^{^5}$ Department of Materials Science and Engineering, The University of Tennessee, Knoxville, Tennessee 37996-2200, USA

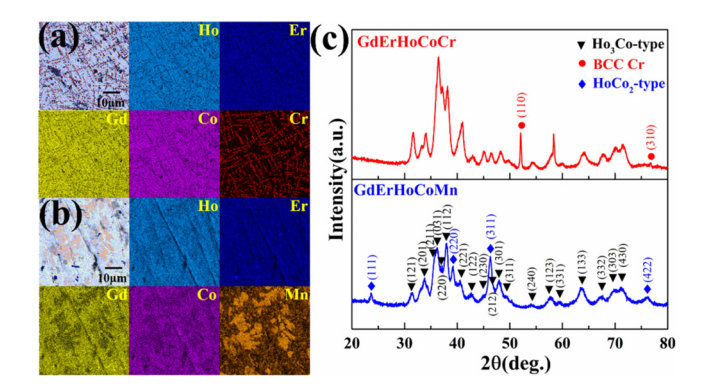


FIG. 1. SEM-EDS micrographs of the GdErHoCoCr (a) and GdErHoCoMn (b) ingots and their XRD patterns (c).

them, the HoErCoAlR (R = Gd, Dy, and Tm) MG-HEA exhibits outstanding comprehensive properties, including magnetic entropy change (11.2 J/kgK), large RC (627 J/kg), and almost no magnetic hysteresis. However, MG-HEAs require rapid cooling during preparation, which limits their size and results in the difficulty of further applications. HeAs The currently known crystalline HEAs with a large MEC are very scarce, which are mainly GdTbHoErLaY¹⁶ series HEAs and FeMnNiGeSi⁹ series HEAs with a hexagonal-close-packed (HCP) structure, the FeNiGaMnSi¹⁰ HEA with a body-centered-cubic (BCC) structure, and the $Mn_{20}Cr_{14}Ni_{33}Ge_{25}Si_8^{19}$ HEA with an orthorhombic structure. Therefore, the development of crystalline RE-HEAs and further magnetic investigation are urgently demanded. In this study, orthorhombic-structured GdErHoCoM (M = Cr and Mn) RE-HEA ingots were developed and analyzed for their magnetic behavior, crystalline structure, and MCE.

The ingots of GdErHoCoM (M=Cr and Mn) were prepared by arc melting with high-purity argon using pure Gd, Er, Ho, Co, Cr, and Mn with a purity over 99.9 wt. %. Before melting, Ti was pre-melted to reduce the oxygen content. The microstructures were studied by Phenom XL scanning electron microscopy (SEM) at an accelerating voltage of 15 keV, and energy-dispersive spectroscopy (EDS) was used to test the compositions. X-ray diffractions (XRD) were measured by a Rigaku Ultima IV diffractometer employing Co-K α radiation at room temperature, and the diffraction angle (2θ) was collected from 20° to

 80° . The magnetic properties were tested by a DynaCoolTM Quantum Design physical property measurement system (PPMS). The thermomagnetic curves were tested at zero field cooling (ZFC) and then field cooling (FC), during which the sample was first cooled without a magnetic field to 2 K, and then the data were collected during heating to 300 K with an applied field of 100 Oe and cooling from 300 to 2 K. The isotherm magnetization curves were measured from 0 to 50 kOe at preset temperatures.

Figure 1 shows the SEM-EDS micrographs and XRD patterns of the GdErHoCoM (M = Cr and Mn) ingots, and further spot analyses on the phases based on 6-10 sites of each phase are summarized in Table I. The SEM micrographs of Figs. 1(a) and 1(b) clearly show that both ingots have two phases. Figure 1(c) presents that the main phase of both ingots is an orthorhombic Ho₃Co-type phase of a space group of Pnma, the first orthorhombic RE-HEA system with a large MEC that has ever been found. Combined with the results of Table I, which exhibits that the percentages of Ho, Er, Gd, and Co are approximately similar, the molecular formula of the main phase in both ingots can be speculated to be (GdErHo)Co. Moreover, in GdErHoCoCr ingots, the morphology of the secondary phase in Fig. 1(a) exhibits a dendritic structure, where the content of Cr is over 94.6 at. %. In the XRD pattern of Fig. 1(c), two diffraction peaks belonging to the (110) and (310) planes of body-center-cubic (BCC) Cr with an Im-3m structure are found at $2\theta = 52.074^{\circ}$ and 76.699° , respectively. Therefore, the secondary phase of GdErHoCoCr ingots can be identified as pure Cr. In GdErHoCoMn ingots, the secondary phase looks like a blocky structure with around 40 at. % of Mn, along with other elements. Three diffraction peaks $(2\theta = 23.627^{\circ}, 39.210^{\circ}, \text{ and } 46.274^{\circ})$ were identified from the HoCo₂-type structure with a C15 cubic structure, in addition to the main phase. It is evident from the SEM-EDS mapping micrographs and XRD peaks that the GdErHoCoMn alloy contains a larger quantity of HoCo2-type phase compared to the GdErHoCoCr alloy. This is indicated by the higher XRD peaks and larger area contents of the HoCo2-type phase in the micrographs. Additionally, the GdErHoCoCr alloy contains BCC Cr.

Figure 2(a) shows the curves of magnetization with temperature (MT) at zero field cooling (ZFC) and field cooling (FC) magnetization of GdErHoCoM (M = Cr and Mn) ingots under a 100 Oe magnetic field in the temperature range from 2 to 300 K. Thermal hysteresis is typically not observed in MT curves, which can prevent energy loss and improve energy utilization during refrigeration cycles. Both ingots

TABLE I. The compositions of different phases by spot analyses of EDS (at. %).

Elements	GdErHoCoCr				GdErHoCoMn			
	Main phase		Secondary phase		Main phase		Secondary phase	
	Mean value	Standard deviation	Mean value	Standard deviation	Mean value	Standard deviation	Mean value	Standard deviation
Cr	0.3	0.2	94.6	3.4				
Mn					3.9	2.9	37.2	6.4
Co	19.1	3.5	1.4	0.6	15.5	1.4	11.1	0.5
Gd	24.0	2.9	0	0	25.6	1.3	6.8	2.8
Но	28.1	1.9	2.5	1.7	28.2	0.8	21.8	0.6
Er	28.7	1.3	1.4	1.2	26.8	1.0	20.1	0.7

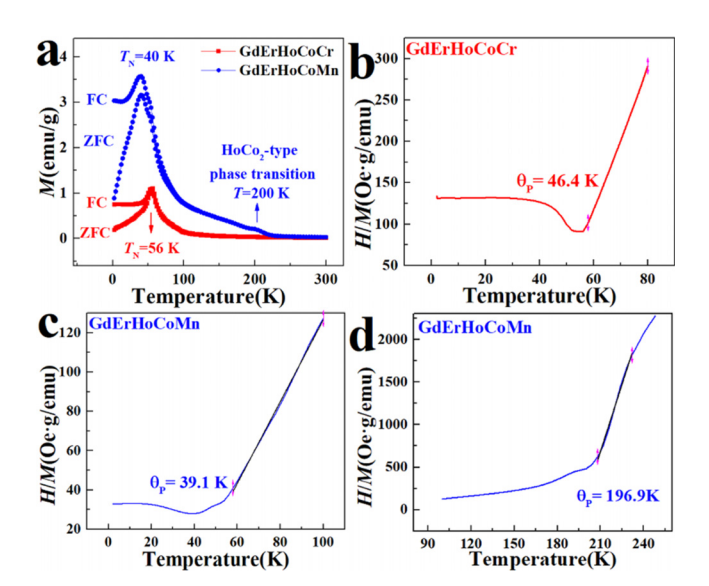


FIG. 2. The *MT* curves at ZFC and FC magnetization (a) and the fitting of χ^{-1} –T by the Curie–Weiss law at 100 Oe of GdErHoCoM (M = Cr and Mn) ingots (b)–(d).

exhibit a typical antiferromagnetic (AFM) to paramagnetic (PM) phase transition, with Neel temperatures (TN) calculated at 40 K for GdErHoCoMn and 56 K for GdErHoCoCr. Another transition near 200 K in the GdErHoCoMn ingot is found. Although the crystal structure of the secondary phase could be identified as a HoCo2-phase by XRD, the exact compositions are complex to confirm due to the severe overlap of the spectral peaks of rare-earth elements in EDS. Additionally, the Curie temperatures of RM₂ (R = Gd, Er, and Ho; M = Co and Mn) alloy range from about 32 to 406 K (32.2 K for ErCo₂, ²⁰ 35 K for GdMn₂, ²¹ 75 K for HoCo₂, ²² and 406 K for GdCo₂ ²³) Based on the available evidence, it is likely that the phase transition occurring around 200 K is related to the HoCo2-type transition. Moreover, an apparent splitting between the ZFC and FC curves is found below their Neel temperatures, indicating that the spin state is sensitive to the external magnetic field. This suggests that the magnetic states differ with or without an external magnetic field. This phenomenon is also observed in the TbDyHoEr alloy.2

Figures 2(b)–2(d) show the fitting of the temperature dependence of the magnetic susceptibility (χ^{-1} –T) curves of GdErHoCoM (M = Cr and Mn) ingots under a field of 100 Oe by the Curie–Weiss law¹⁶

$$\chi^{-1} = \frac{T - \theta_P}{C},\tag{1}$$

where χ^{-1} is the reciprocal of magnetic susceptibility, T is the temperature, θ_P is the paramagnetic Curie temperature, and C is the Curie constant. The paramagnetic Curie temperature in the high-temperature range near $T_{\rm N}$ for the GdErHoCoM (M=Cr and Mn) is found $\theta_P=46.4$ and $\theta_P=39.1$ K, respectively. In the GdErHoCoMn ingot near 200 K, the χ^{-1} -T curve has another positive θ_P , that is, 196.9 K. Typically, the value of θ_P of the antiferromagnet is negative, ^{25–28} and the positive value of θ_P is rarely reported. ^{29,30} The positive values of θ_P of the GdErHoCoM (M=Cr and Mn) ingots may be ascribed to the instability of AFM under a large magnetic field, resulting in the ferromagnetic (FM) interaction in the two ingots.

Figures 3(a) and 3(b) present the magnetization (MH) curves of the GdErHoCoM (M = Cr and Mn) ingots at the applied magnetic field of 5 T with a wide temperature range from 5 to 200 K and from 5 to 250 K for GdErHoCoCr and GdErHoCoMn, respectively. It could be found that with the increased magnetic field, the saturation magnetic moment decreases in both ingots. Yet generally, the saturation magnetic moment of the GdErHoCoCr ingot is larger than that of the GdErHoCoMn ingot at the same temperature. Moreover, the magnetization of the two ingots gradually approaches saturation, showing a ferromagnetic feature at low temperatures below T_N . While at high temperatures above T_N , the MH curves gradually turn to straight lines with the increase in temperature, indicating a transition from a magnetic order to disorder,³¹ showing a paramagnetic feature. Figures 3(c)-3(d) show the enlarged curves of Figs. 3(a) and 3(b) from 0 to 2 T below T_N . It could be seen that the initial magnetization curves experience a nonlinearly sharp increase at the initial stage and then reach

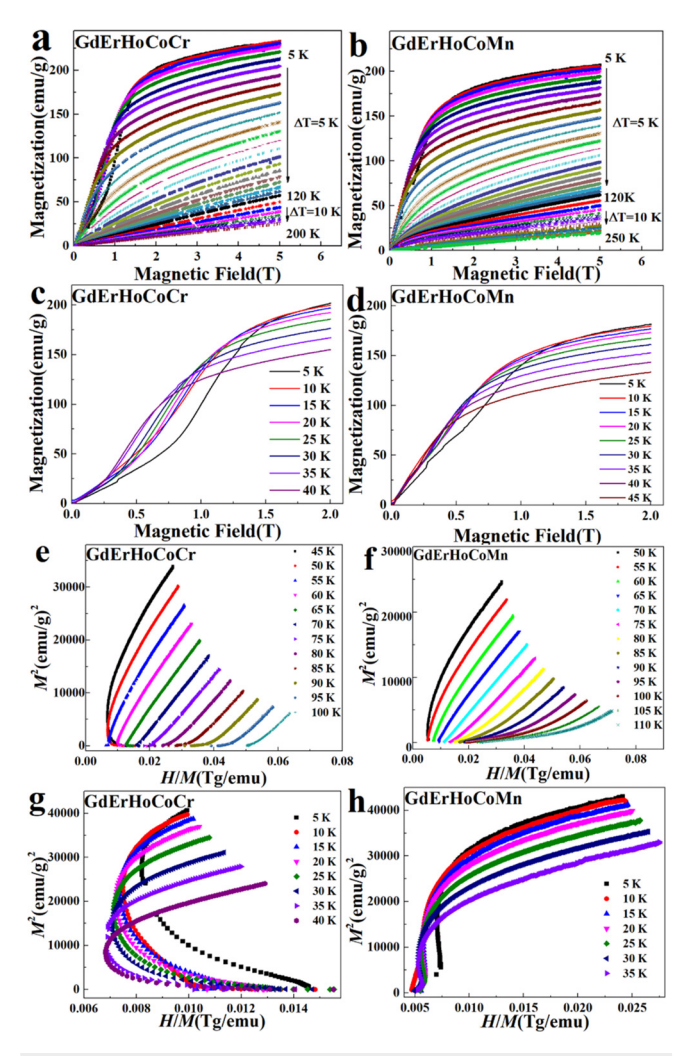


FIG. 3. Isothermal magnetization (MH) curves of GdErHoCoM (M = Cr and Mn) ingots at different temperatures from 0–5 T (a) and (b) and their enlarged images from 0–2 T (c) and (d); Arrott curves above (e) and (f) and below (g) and (h) T_N .

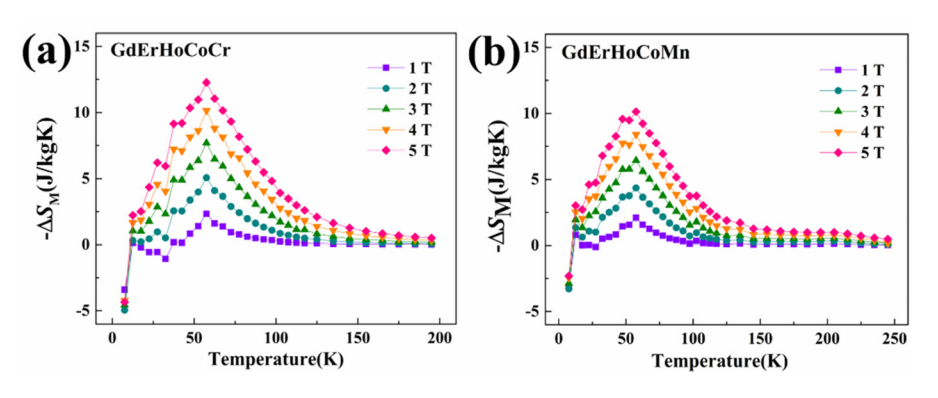


FIG. 4. The curves of the dependence of magnetic entropy change on temperature $[(-\Delta S_{\rm M})-{\rm T}]$ of GdErHoCoCr (a) and GdErHoCoMn ingots (b).

their saturation, indicating that the metamagnetic transition below $T_{\rm N}$ is from AFM to FM induced by the external magnetic field, which leads to the split in Fig. 2(a) below $T_{\rm N}$. The Arrott curves above $T_{\rm N}$, as shown in Figs. 3(e) and 3(f) present positive slopes, and there is a second-order magnetic phase transition (SOMT) from AFM to PM in both ingots. The Arrott curves below $T_{\rm N}$ are presented in Figs. 3(g) and 3(h). The S-shape curves or negative slopes indicate that the phase transition from AFM to PM below $T_{\rm N}$ is the first-order magnetic phase transition (FOMT) 32 induced by the magnetic field.

The isothermal magnetic entropy change (ΔS_{M}), a key parameter to judge the magnetic cooling capacity, is calculated from the isothermal magnetization curves by the Maxwell equation of the two ingots, as follows:³³

$$\Delta S_{M}(T,H) = \int_{H_{0}}^{H_{max}} \left(\frac{\partial M}{\partial T}\right)_{H} dH, \tag{2}$$

where M is the magnetization, T is the temperature, H is the magnetic field, and H_0 and H_{max} are the initial and final values of the magnetic field, respectively. Here, $H_0=0$ and $H_{max}=5$ T. To obtain the values of ΔS_M , the numerical approximation is used³⁴

$$\Delta S_M(T_i, H_k) = \sum_{i=0}^{j=k-1} \frac{M(T_{i+1}, H_j) - M(T_i, H_j)}{T_{i+1} - T_i} (H_{j+1} - H_j), \quad (3)$$

where $M(T_i, H_j)$ is the magnetization at a temperature, T_i , under a magnetic field, H_j . The error of the values of ΔS_M is less than 7% by numerical approximation.³⁵

The $(-\Delta S_M)$ -T curves of GdErHoCoM ingots are presented in Fig. 4. It is an abnormal phenomenon that the value of $-\Delta S_{\rm M}$ of the two ingots is negative at low temperatures under the applied field of 1 T, which originates from the metamagnetic transitions, as shown in Figs. 3(c) and 3(d). The negative value of $-\Delta S_{\rm M}$ indicates that the sample cools when a magnetic field is applied and heats up when the magnetic field is removed. In contrast, a positive $-\Delta S_{\mathrm{M}}$ value results in a sample being heated in the presence of a magnetic field and cooled in its absence. As the increase in temperature, the value of $-\Delta S_{\rm M}$ increases, reaching a maximum around the Curie temperature, and then decreases. The maximum values of the magnetic entropy change of GdErHoCoM (M = Cr and Mn) ingots are 12.29 and 10.13 J/kg/K at 57.5 K under 5 T, respectively. Moreover, the larger maximum of $-\Delta S_{\rm M}$ of the GdErHoCoCr originates from a larger saturation magnetic moment of the GdErHoCoCr ingot, as shown in Figs. 3(a) and 3(b). In addition, the maximum of $-\Delta S_{\rm M}$ values of the GdErHoCoCr ingots is higher than most known crystalline HEAs, $^{10,14,16,17,24,36-38}$ MG-HEAs, $^{13,15,24,33,39-55}$ and only 22.8% lower than 15.91 J/kg/K of the known highest $\rm Er_{50}Co_{20}Al_{24}Y_6$ MG-HEA, 56 indicating its great potential for the magnetic refrigeration applications.

The *RC* is another critical parameter to evaluate the magnetic refrigeration capacity and can be calculated by⁵⁷

$$RC = -\Delta S_M^{max} \times \delta T_{FWHW}, \tag{4}$$

where $-\Delta S_M^{max}$ is the maximum value of the magnetic entropy change and δT_{FWHW} is the width at half maximum of $-\Delta S_M$ in $(-\Delta S_M)$ -T curve. The RC values of GdErHoCoM (M = Cr and Mn) ingots could be calculated to reach 746 and 606 J/kg, respectively.

Figure 5 presents the RC vs $|\Delta S_{\rm M}|_{\rm max}$ of the most known MEC-HEAs under a field of 5 T that have ever been reported. On the suitable for magnetic refrigeration applications, materials must have large RC and $|\Delta S_{\rm M}|_{\rm max}$ values and, thus, be located closer to the upper right corner of the relevant graph. It can be observed that the GdErHoCoM ingots, and particularly the GdErHoCoCr ingots, have great RC and $|\Delta S_{\rm M}|_{\rm max}$ synergy when compared to most crystalline HEAs and MG-HEAs. Based on the composition in the present work, further optimization in the chemical composition, phase

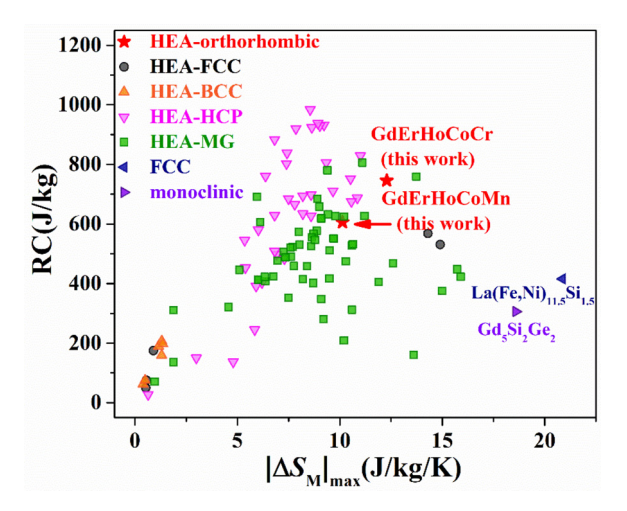


FIG. 5. MCE performance of RC vs $|\Delta S_{\rm M}|_{\rm max}$ of the most known HEAs and typical crystal alloys [an fcc structure of La(Fe, Ni)_{11.5}Si_{1.5} and monoclinic structure of Ge₅Si₂Ge₂] under a field of 5 T. Literature data were collected from Refs. 10, 13–17, 24, 33, 36–56, and 58–79.

composition, and heat treatment can still be taken for further property elevation. Moreover, the manufacturing process of the GdErHoCoM ingot is more straightforward than that of the melted ribbons in many crystalline HEAs and rapid cooling in MG-HEAs. The large MCE values, as well as the simple ingot manufacturing process, make GdErHoCoM (M = Cr and Mn) ingots potential candidates for magnetic refrigeration applications.

In summary, orthorhombic GdErHoCoM (M = Cr and Mn) RE-HEAs with the giant MCE were developed, and their magnetic behavior, as well as the magnetocaloric effect of GdErHoCoM (M = Cr and Mn) HEA ingots, was studied in detail. The main findings include

- The main phases of both ingots are orthorhombic Ho₃Co-type structures of a space group of Pnma, and their formula probably is (GdErHo)Co. The secondary phases of GdErHoCoCr and GdErHoCoMn are pure Cr- and Mn-rich HoCo₂-type structures, respectively.
- GdErHoCoCr and GdErHoCoMn ingots undergo a first-order magnetic phase transition below their respective Neel temperatures and a second-order magnetic transition above them, with no thermal hysteresis. The Neel temperature is 40 K for GdErHoCoCr and 56 K for GdErHoCoMn.
- 3. The ingots of GdErHoCoCr and GdErHoCoMn exhibit $-\Delta S_{\rm M}$ and RC values of 12.29 J/kg/K and 746 J/kg and 10.13 J/kg/K and 606 J/kg, respectively, under 5 T. Due to their excellent RC and $|\Delta S_{\rm M}|_{\rm max}$ synergy, coupled with a simple manufacturing process, the GdErHoCoM (M=Cr and Mn) ingots hold potential as strong candidates for use in magnetic refrigeration applications.

This work was supported by the Fundamental Research Program of Shanxi Province (Nos. 20210302124535, 20210302124043, and 202203021212304), the Shanxi Scholarship Council of China, the special fund for Science and Technology Innovation Teams of Shanxi Province (No. 202304051001036). P.K. L. very much appreciates the support from (1) the National Science Foundation (DMR—Nos. 1611180, 1809640, and 2226508) and (2) the Army Research Office (Nos. FA9550-23-1-0503, W911NF-13-1-0438, and W911NF-19-2-0049).

AUTHOR DECLARATIONS Conflict of Interest

The authors have no conflicts to disclose.

Author Contributions

Xuejiao Wang: Formal analysis (equal); Funding acquisition (equal); Investigation (equal); Methodology (equal); Visualization (equal); Writing – original draft (equal); Writing – review & editing (equal). Shuotong Zong: Conceptualization (equal); Formal analysis (equal); Funding acquisition (equal); Investigation (equal); Methodology (equal); Validation (equal); Writing – original draft (equal); Writing – review & editing (equal). Yan Zhang: Formal analysis (equal); Funding acquisition (equal); Investigation (equal); Validation (equal). Zhaojun Mo: Data curation (equal); Formal analysis (equal); Investigation (equal); Methodology (equal). Junwei Qiao: Conceptualization (equal); Formal analysis (equal); Visualization (equal); Writing – original draft (equal); Writing – review & editing

(equal). **Peter K. Liaw:** Visualization (equal); Writing – review & editing (equal).

DATA AVAILABILITY

The data that support the findings of this study are available from the corresponding authors upon reasonable request.

REFERENCES

- B. G. Shen, J. R. Sun, F. X. Hu, H. W. Zhang, and Z. H. Cheng, "Recent progress in exploring magnetocaloric materials," Adv. Mater. 21(45), 4545–4564 (2009).
 V. K. Pecharsky and K. A. Gschneidner, Jr., in Advances in Cryogenic
- Engineering (Springer, 1998), pp. 1729–1736.
- ³K. A. Gschneidner, Jr. and V. K. Pecharsky, "Magnetocaloric materials," Annu. Rev. Mater. Sci. 30(1), 387–429 (2000).
 ⁴A. Kitanovski and P. W. Egolf, "Thermodynamics of magnetic refrigeration,"
- Int. J. Refrig. **29**(1), 3–21 (2006).
 ⁵O. Sari and M. Balli, "From conventional to magnetic refrigerator technology,"
- Int. J. Refrig. 37, 8–15 (2014).

 ⁶X. Chang, M. Zeng, K. Liu, and L. Fu, "Phase engineering of high-entropy
- alloys," Adv. Mater. 32(14), 1907226 (2020).
 P. George, D. Raabe, and R. O. Ritchie, "High-entropy alloys," Nat. Rev. Mater. 4(8), 515–534 (2019).
- ⁸H. Tanimoto, R. Hozumi, and M. Kawamura, "Electrical resistivity and short-range order in rapid-quenched CrMnFeCoNi high-entropy alloy," J. Alloys Compd. 896, 163059 (2022).
- ⁹J. Y. Law, Á. Díaz-García, L. M. Moreno-Ramírez, and V. Franco, "Increased magnetocaloric response of FeMnNiGeSi high-entropy alloys," Acta Mater. 212, 116931 (2021).
- ¹⁰K. Sarlar, A. Tekgül, and I. Kucuk, "Magnetocaloric properties in a FeNiGaMnSi high entropy alloy," Curr. Appl. Phys. 20(1), 18–22 (2020).
- ¹¹Y. Zhang, J. Zhu, Z. Hao, W. Hao, Z. Mo, and L. Li, "Tunable magnetic phase transition and magnetocaloric effect in the rare-earth-free Al-Mn-Fe-Co-Cr high-entropy alloys," Mater. Des. 229, 111894 (2023).
- ¹²J. Y. Law, L. M. Moreno-Ramírez, Á. Díaz-García, A. Martín-Cid, S. Kobayashi, S. Kawaguchi, T. Nakamura, and V. Franco, "MnFeNiGeSi high-entropy alloy with large magnetocaloric effect," J. Alloys Compd. 855, 157424 (2021).
- ¹³J. Huo, L. Huo, J. Li, H. Men, X. Wang, A. Inoue, C. Chang, J.-Q. Wang, and R.-W. Li, "High-entropy bulk metallic glasses as promising magnetic refrigerants," J. Appl. Phys. 117(7), 073902 (2015).
- 14.Y. Yuan, Y. Wu, X. Tong, H. Zhang, H. Wang, X. J. Liu, L. Ma, H. L. Suo, and Z. P. Lu, "Rare-earth high-entropy alloys with giant magnetocaloric effect," Acta Mater. 125, 481–489 (2017).
- 15W. Sheng, J.-Q. Wang, G. Wang, J. Huo, X. Wang, and R.-W. Li, "Amorphous microwires of high entropy alloys with large magnetocaloric effect," Intermetallics 96, 79–83 (2018).
- ¹⁶S. F. Lu, L. Ma, J. Wang, Y. S. Du, L. Li, J. T. Zhao, and G. H. Rao, "Effect of configuration entropy on magnetocaloric effect of rare earth high-entropy alloy," J. Alloys Compd. 874, 159918 (2021).
- ¹⁷S. A. Uporov, S. K. Estemirova, E. V. Sterkhov, I. A. Balyakin, and A. A. Rempel, "Magnetocaloric effect in ScGdTbDyHo high-entropy alloy: Impact of synthesis route," Intermetallics 151, 107678 (2022).
- ¹⁸W.-H. Wang, C. Dong, and C. H. Shek, "Bulk metallic glasses," Mater. Sci. Eng. R 44(2-3), 45-89 (2004).
- ¹⁹A. Tekgül, K. Sarlar, N. Küçük, and A. B. Etemoğlu, "The structural, magnetic and magnetocaloric properties of MnCrNiGeSi high-entropy alloy," Phys. Scr. 97(7), 075814 (2022).
- 20 H. Wada, S. Tomekawa, and M. Shiga, "Magnetocaloric properties of a first-order magnetic transition system ErCo₂," Cryogenics 39(11), 915–919 (1999)
- ²¹J. S. Marcos, J. R. Fernández, B. Chevalier, J.-L. Bobet, and J. Etourneau, "Heat capacity and magnetocaloric effect in polycrystalline and amorphous GdMn₂," J. Magn. Magn. Mater. 272–276, 579–580 (2004).
- ²²J. Voiron, A. Berton, and J. Chaussy, "Specific heat and induced moment in HoCo₂ and TbCo₂," Phys. Lett. A 50(1), 17–19 (1974).

- ²³Z. Gu, B. Zhou, J. Li, W. Ao, G. Cheng, and J. Zhao, "Magnetocaloric effect of GdCo_{2-x}Al_x compounds," Solid State Commun. 141(10), 548-550 (2007).
- ²⁴W. H. Zhu, L. Ma, M. F. He, Z. K. Li, H. Z. Zhang, Q. R. Yao, G. H. Rao, K. P. Su, X. C. Zhong, and Z. W. Liu, "Large refrigerant capacity induced by table-like magnetocaloric effect in high-entropy alloys TbDyHoEr," Adv. Eng. Mater. 25(11), 2201770 (2023).
- ²⁵Y. Zhang, Y. Tian, Z. Zhang, Y. Jia, B. Zhang, M. Jiang, J. Wang, and Z. Ren, "Magnetic properties and giant cryogenic magnetocaloric effect in B-site ordered antiferromagnetic Gd₂MgTiO₆ double perovskite oxide," Acta Mater. 226, 117669 (2022).
- ²⁶M. Das, S. Roy, N. Khan, and P. Mandal, "Giant magnetocaloric effect in an exchange-frustrated GdCrTiO₅ antiferromagnet," Phys. Rev. B 98(10), 104420 (2018).
- ²⁷A. Boutahar, R. Moubah, E. K. Hlil, H. Lassri, and E. Lorenzo, "Large reversible magnetocaloric effect in antiferromagnetic Ho₂O₃ powders," Sci. Rep. 7(1), 13904 (2017).
- ²⁸Q. Y. Dong, K. Y. Hou, X. Q. Zhang, L. Su, L. C. Wang, Y. J. Ke, H. T. Yan, and Z. H. Cheng, "Giant reversible magnetocaloric effect in antiferromagnetic rareearth cobaltite GdCoO₃," J. Appl. Phys. 127(3), 033904 (2020).
- ²⁹H. Zhang, Y. Wu, Y. Long, H. Wang, K. Zhong, F. Hu, J. Sun, and B. Shen, "Large reversible magnetocaloric effect in antiferromagnetic HoNiSi compound," J. Appl. Phys. 116(21), 213902–213905 (2014).
- ³⁰J. Chen, B. G. Shen, Q. Y. Dong, F. X. Hu, and J. R. Sun, "Giant reversible magnetocaloric effect in metamagnetic HoCuSi compound," Appl. Phys. Lett. 96(15), 152501 (2010).
- ³¹Z. Shuotong, L. Yi, G. Qi, Z. Kewei, C. Fenghua, and H. Jifan, "Critical behavior of the second-order magnetic transition in LaFe_{11.7-x}Co_xSi_{1.3}C_{0.15} alloys," J. Magn. Magn. Mater. 547, 168932 (2022).
- 32 S. T. Zong and Y. Long, "The influence of Cr and Ni on the character of magnetic phase transition in LaFe_{11.52-x}M_xSi_{1.48} alloys," AIP Adv. 8(4), 048101 (2018).
- ³³Q. Luo, D. Q. Zhao, M. X. Pan, and W. H. Wang, "Magnetocaloric effect in Gd-based bulk metallic glasses," Appl. Phys. Lett. 89(8), 081914 (2006).
- 34A. Guzik, E. Talik, and P. Zajdel, "Magnetocaloric effect of the Gd_{3-x}Tb_xCo system," Intermetallics 118, 106686 (2020).
- 35M. Földeàki, R. Chahine, and T. K. Bose, "Magnetic measurements: A powerful tool in magnetic refrigerator design," J. Appl. Phys. 77(7), 3528-3537 (1995)
- ³⁶S. F. Lu, L. Ma, G. H. Rao, J. Wang, Y. S. Du, L. Li, J. T. Zhao, X. C. Zhong, and Z. W. Liu, "Magnetocaloric effect of high-entropy rare-earth alloy GdTbHoEry," J. Mater. Sci. 32, 10919–10926 (2021).
- ³⁷S. Uporov, E. Sterkhov, and I. Balyakin, "Magnetocaloric effect in ScGdHo medium-entropy alloy," J. Supercond. Nov. Magn. 35, 1539–1545 (2022).
- ³⁸L. Wang, Z. Lu, Y. Wu, Y. Zhang, R. Zhao, S. Jiang, X. Liu, H. Wang, D. Ma, and Z. Lu, "Effect of Sc addition on magnetocaloric properties of GdTbDyHo high-entropy alloys," Adv. Eng. Mater. 26, 2300616 (2023).
- ³⁹L. Li, C. Xu, Y. Yuan, and S. Zhou, "Large refrigerant capacity induced by table-like magnetocaloric effect in amorphous Er_{0.2}Gd_{0.2}Ho_{0.2}Co_{0.2}Cu_{0.2} ribbons," Mater. Res. Lett. 6(8), 413–418 (2018).
- ⁴⁰F. Yuan, J. Du, and B. Shen, "Controllable spin-glass behavior and large magne-tocaloric effect in Gd-Ni-Al bulk metallic glasses," Appl. Phys. Lett. 101(3), 032405 (2012).
- ⁴¹J. Du, Q. Zheng, E. Brück, K. H. J. Buschow, W. B. Cui, W. J. Feng, and Z. D. Zhang, "Spin-glass behavior and magnetocaloric effect in Tb-based bulk metallic glass," J. Magn. Magn. Mater. 321(5), 413–417 (2009).
- ⁴²L. Liang, X. Hui, Y. Wu, and G. L. Chen, "Large magnetocaloric effect in Gd₃₆Y₂₀Al₂₄Co₂₀ bulk metallic glass," J. Alloys Compd. 457(1–2), 541–544 (2008).
- ⁴³Y. Zhang, B. Wu, D. Guo, J. Wang, and Z. Ren, "Magnetic properties and promising cryogenic magneto-caloric performances of Gd₂₀Ho₂₀Tm₂₀Cu₂₀Ni₂₀ amorphous ribbons," Chin. Phys. B 30(1), 017501 (2021).
- ⁴⁴C. M. Pang, L. Chen, H. Xu, W. Guo, Z. W. Lv, J. T. Huo, M. J. Cai, B. L. Shen, X. L. Wang, and C. C. Yuan, "Effect of Dy, Ho, and Er substitution on the magnetocaloric properties of Gd-Co-Al-Y high entropy bulk metallic glasses," J. Alloys Compd. 827, 154101 (2020).
- ⁴⁵J. Huo, J.-Q. Wang, and W.-H. Wang, "Denary high entropy metallic glass with large magnetocaloric effect," J. Alloys Compd. 776, 202–206 (2019).

- ⁴⁶L. Luo, H. Shen, Y. Bao, H. Yin, S. Jiang, Y. Huang, S. Guo, S. Gao, D. Xing, and Z. Li, "Magnetocaloric effect of melt-extracted high-entropy Gd₁₉Tb₁₉Er₁₈Fe₁₉Al₂₅ amorphous microwires," J. Magn. Magn. Mater. **507**, 166856 (2020).
- ⁴⁷K. Wu, C. Liu, Q. Li, J. Huo, M. Li, C. Chang, and Y. Sun, "Magnetocaloric effect of Fe₂₅Co₂₅Ni₂₅Mo₅P₁₀B₁₀ high-entropy bulk metallic glass," J. Magn. Magn. Mater. 489, 165404 (2019).
- ⁴⁸C. Liu, Q. Li, J. Huo, W. Yang, L. Chang, C. Chang, and Y. Sun, "Near room-temperature magnetocaloric effect of Co-based bulk metallic glass," J. Magn. Magn. Mater. 446, 162–165 (2018).
- ⁴⁹L. Liang, X. Hui, C. M. Zhang, and G. L. Chen, "A Dy-based bulk metallic glass with high thermal stability and excellent magnetocaloric properties," J. Alloys Compd. 463(1–2), 30–33 (2008).
- 50 J. Li, L. Xue, W. Yang, C. Yuan, J. Huo, and B. Shen, "Distinct spin glass behavior and excellent magnetocaloric effect in Er₂₀Dy₂₀Co₂₀Al₂₀RE₂₀ (RE= Gd, Tb and Tm) high-entropy bulk metallic glasses," Intermetallics 96, 90–93 (2018).
- 51]. Huo, L. Huo, H. Men, X. Wang, A. Inoue, J. Wang, C. Chang, and R. W. Li, "The magnetocaloric effect of Gd-Tb-Dy-Al-M (M=Fe, Co and Ni) high-entropy bulk metallic glasses," <u>Intermetallics</u> 58, 31–35 (2015).
- ⁵²L. Xue, L. Shao, Q. Luo, and B. Shen, "Gd₂₅RE₂₅Co₂₅Al₂₅ (RE= Tb, Dy and Ho) high-entropy glassy alloys with distinct spin-glass behavior and good magnetocaloric effect," J. Alloys Compd. **790**, 633–639 (2019).
- ⁵³L. Xue, L. Shao, Z. Li, Z. Han, B. Zhang, J. Huo, X. Wang, S. Zhu, B. Qian, and J. Cheng, "Utilization of high entropy in rare earth-based magnetocaloric metallic glasses," J. Mater. Res. Technol. 18, 5301–5311 (2022).
- 54C. M. Pang, C. C. Yuan, L. Chen, H. Xu, K. Guo, J. C. He, Y. Li, M. S. Wei, X. M. Wang, and J. T. Huo, "Effect of Yttrium addition on magnetocaloric properties of Gd-Co-Al-Ho high entropy metallic glasses," J Non-Cryst. Solids 549, 120354 (2020).
- 55M. Cai, Q. Luo, Q. Zeng, and B. Shen, "Combined effect of demagnetization field and magnetic anisotropy on magnetocaloric behavior and magnetocaloric-magnetoresistance correlation in GdTmErCoAl high-entropy amorphous alloy," J. Magn. Magn. Mater. 528, 167817 (2021).
- ⁵⁶Q. Luo, D. Q. Zhao, M. X. Pan, and W. H. Wang, "Magnetocaloric effect of Ho-, Dy-, and Er-based bulk metallic glasses in helium and hydrogen liquefaction temperature range," Appl. Phys. Lett. 90(21), 211903 (2007).
- ⁵⁷L. Li, Y. Yuan, Y. Zhang, T. Namiki, K. Nishimura, R. Pöttgen, and S. Zhou, "Giant low field magnetocaloric effect and field-induced metamagnetic transition in TmZn," Appl. Phys. Lett. **107**(13), 132401 (2015).
- ⁵⁸Z. Dong, Z. Wang, and S. Yin, "Magnetic properties and large cryogenic magneto-caloric effect of Er_{0.2}Tm_{0.2}Ho_{0.2}Cu_{0.2}Co_{0.2} amorphous ribbon," Intermetallics 124, 106879 (2020).
- 59V. K. Pecharsky and K. A. Gschneidner, Jr., "Giant magnetocaloric effect in Gd₅(Si₂Ge₂)," Phys. Rev. Lett. 78(23), 4494 (1997).
- ⁶⁰G. Cao, Q. Wang, J. Liu, Y. Zhang, X. Wang, M. Huang, H. Shen, and L. Zheng, "Enhanced magnetic entropy change and refrigeration capacity of La (Fe,Ni)_{11.5}Si_{1.5} alloys through vacuum annealing treatment," J. Alloys Compd. 800, 363–371 (2019).
- ⁶¹Y. Zhang, P. Xu, J. Zhu, S. Yan, J. Zhang, and L. Li, "The emergence of considerable room temperature magnetocaloric performances in the transition metal high-entropy alloys," Mater. Today Phys. 32, 101031 (2023).
- ⁶²L. Shao, L. Xue, Q. Luo, K. Yin, Z. Yuan, M. Zhu, T. Liang, Q. Zeng, L. Sun, and B. Shen, "Heterogeneous GdTbDyCoAl high-entropy alloy with distinctive magnetocaloric effect induced by hydrogenation," J. Mater. Sci. Technol. 109, 147–156 (2022).
- 63L. Xue, Q. Luo, L. Shao, and B. Shen, "Magnetocaloric difference between ribbon and bulk shape of Gd-based metallic glasses," J. Magn. Magn. Mater. 497, 166015 (2020)
- ⁶⁴F. Jin, C. Yuan, C. Pang, X. Wang, C. Cao, and J. Huo, "Entropy tailoring of thermodynamic behaviors and magnetocaloric effects in (GdTbDy)CoAl metallic glasses," Mater. Des. 238, 112653 (2024).
- 65Z. Dong, Z. Wang, and S. Yin, "Magnetic properties and magneto-caloric effect (MCE) in Cu₂₂Al₁₈Ho₂₂Tm₂₀Gd₁₈ amorphous ribbons," J. Magn. Magn. Mater. 514, 167270 (2020).
- ⁶⁶S.-J. Wei, H.-X. Shen, L.-Y. Zhang, L. Luo, X.-X. Tang, J.-F. Sun, and X.-Q. Li, "Microstructure and magnetocaloric properties of melt-extracted

- SmGdDyCoAl high-entropy amorphous microwires," Rare Met. 43, 1234-1242 (2024).
- 67 K. Wu, C. Liu, Q. Li, J. Huo, and Y. Sun, "Study on mangnetocaloric effect of Fe25Co25Ni25CrSP10810 high entropy bulk amorphous alloy," J. Funct. Mater. 50(5), 5095–5098 (2019).
- ⁶⁸H. Yin, J. Law, Y. Huang, V. Franco, H. Shen, S. Jiang, Y. Bao, and J. Sun, "Design of Fe-containing GdTbCoAl high-entropy-metallic-glass composite microwires with tunable Curie temperatures and enhanced cooling efficiency," Mater. Des. 206, 109824 (2021).
- ⁶⁹H. Yin, J. Y. Law, Y. Huang, H. Shen, S. Jiang, S. Guo, V. Franco, and J. Sun, "Enhancing the magnetocaloric response of high-entropy metallic-glass by microstructural control," Sci. China Mater. 65(4), 1134–1142 (2022).
- 70 H. Yin, J.-Q. Wang, Y. Huang, H. Shen, S. Guo, H. Fan, J. Huo, and J. Sun, "Relating microstructure to magnetocaloric properties in RE₃₆Tb₂₀Co₂₀Al₂₄ (RE = Gd, Dy or Ho) high-entropy metallic-glass microwires designed by binary eutectic clusters method," J. Mater. Sci. Technol. 149, 167–176 (2023).
- ⁷¹Y. Zhang, J. Zhu, S. Li, J. Wang, and Z. Ren, "Achievement of giant cryogenic refrigerant capacity in quinary rare-earths based high-entropy amorphous alloy," J. Mater. Sci. Technol. 102, 66–71 (2022).
- 72A. Quintana-Nedelcos, Z. Leong, and N. A. Morley, "Study of dual-phase functionalisation of NiCoFeCr-Al_x multicomponent alloys for the enhancement of magnetic properties and magneto-caloric effect," Mater. Today Energy 20, 100621 (2021).

- ⁷³D. D. Belyea, M. S. Lucas, E. Michel, J. Horwath, and C. W. Miller, "Tunable magnetocaloric effect in transition metal alloys," Sci. Rep. 5(1), 15755 (2015).
- 74P. K. Jesla, J. Arout Chelvane, and R. Nirmala, "Estimation of magnetocaloric effect in multicomponent material Gd_{0.2}Tb_{0.2}Dy_{0.2}Ho_{0.2}Er_{0.2}Ni₂: Exploring high-entropy design," J. Magn. Magn. Mater. 590, 171651 (2024).
- 75S. Vorobiov, O. Pylypenko, Y. Bereznyak, I. Pazukha, E. Čižmár, M. Orendáč, and V. Komanicky, "Magnetic properties, magnetoresistive, and magnetocaloric effects of AlCrFeCoNiCu thin-film high-entropy alloys prepared by the co-evaporation technique," Appl. Phys. A 127(3), 179 (2021).
- ⁷⁶W. H. Zhu, L. Ma, M. F. He, S. F. Lu, Z. K. Li, G. H. Rao, L. Li, X. M. Li, and C. Q. Yin, "Magnetic properties and magnetocaloric effect of GdTbHoEr-based high-entropy alloy ribbons," J. Mater. Sci. 33(34), 25930–25938 (2022).
- ⁷⁷L. Xue, L. Shao, B. Zhang, Z. Li, J. Cheng, and B. Shen, "Magnetic behaviors and magnetocaloric effects in rare earth high-entropy amorphous/nanocrystal-line alloys," J. Rare Earths 42(1), 129–136 (2024).
- ⁷⁸L. Wang, Z. Lu, H. Guo, Y. Wu, Y. Zhang, R. Zhao, S. Jiang, X. Liu, H. Wang, Z. Fu, J. Zhao, D. Ma, and Z. Lu, "Multi-principal rare-earth Gd-Tb-Dy-Ho-Er alloys with high magnetocaloric performance near room temperature," J. Alloys Compd. 960, 170901 (2023).
- 79S. A. Uporov, E. V. Sterkhov, I. A. Balyakin, V. A. Bykov, I. S. Sipatov, and A. A. Rempel, "Synthesis and magnetic properties of some monotectic composites containing ultra-dispersed particles of YGdTbDyHo high-entropy alloy," Intermetallics 165, 108121 (2024).